# RGB Calibration for Color Image Analysis in Machine Vision

Young-Chang Chang, *Member, IEEE*, and John F. Reid, *Member, IEEE*

***Abstract*—A color calibration method for correcting the variations in RGB color values caused by vision system components was developed and tested in this study. The calibration scheme concentrated on comprehensively estimating and removing the RGB errors without specifying error sources and their effects. The algorithm for color calibration was based upon the use of a standardized color chart and developed as a preprocessing tool for color image analysis. According to the theory of image formation, RGB errors in color images were categorized into multiplicative and additive errors. Multiplicative and additive errors contained various error sources—gray-level shift, a variation in amplification and quantization in camera electronics or frame grabber, the change of color temperature of illumination with time, and related factors. The RGB errors of arbitrary colors in an image were estimated from the RGB errors of standard colors contained in the image. The color calibration method also contained an algorithm for correcting the nonuniformity of illumination in the scene. The algorithm was tested under two different conditions—uniform and nonuniform illumination in the scene. The RGB errors of arbitrary colors in test images were almost completely removed after color calibration. The maximum residual error was seven gray levels under uniform illumination and 12 gray levels under nonuniform illumination. Most residual RGB errors were caused by residual nonuniformity of illumination in images. The test results showed that the developed method was effective in correcting the variations in RGB color values caused by vision system components.**

## I. INTRODUCTION

ONE OF many difficulties in dealing with color images in machine vision applications results from variations in RGB color values caused by vision system components. Tappen *et al.* [1] identified a number of error sources from equipment in digital image analysis, such as auto black circuits and the change in gray-scale range. Spomer and Smith [2] pointed out the variations in quantitative RGB data introduced by the camera residual autogain when the camera autogain was turned off. Tao *et al.* [3] noticed that the lighting intensity was changed with time during machine vision inspection of potatoes. Ahmad and Reid [4] reported that the RGB values of reference colors used for color analysis of corn stress had changed in every image. Without calibrating the color information distorted by vision system components, the results of color image analysis may conceal or inaccurately represent important color characteristics of objects in images.

Manuscript received August 17, 1994; revised November 27, 1995. The associate editor coordinating the review of this paper and approving it for publication was Prof. Rama Chellappa.

The authors are with the Department of Agricultural Engineering, University of Illinois at Urbana-Champaign, Urbana, IL 61801 USA (e-mail: cyc9840@sugar.age.uiuc.edu).

Publisher Item Identifier S 1057-7149(96)05254-2.

For intensity image analysis, there have been a few studies to reduce the errors caused by vision system components. The intensity nonlinearity resulting from the image sensor was corrected by the lookup table using programmable ROM [5]. McClellan [6] corrected the change of camera transfer function caused by the gray-level shift, defined as the change of gray level with the average image illuminance. The correction results showed that the gray-level shift was reduced to less than 2% of 255 full scale. Also, he suggested that better results would be obtained by individually characterizing the gray-level shift for each pixel.

Crowther and Neale [7] performed the correction of lens vignetting effects and sensor array nonuniformities. Their correction strategy was to obtain the ratios of the brightness of pixels to the average brightness on the middle area of Lambertian reflectance panel imagery. Then, the brightness of the image acquired at a particular lens aperture was multiplied by those ratios. The correction was separately conducted for red, green, and infrared images.

Some researchers have tried to analytically remove the variation in illumination. The most common study was the color constancy meaning the recovery of surface color, independent of the color of illumination, from the RGB responses of a camera [8], [9]. Shio [10] derived an illumination-independent contrast measure. He showed that the contrast measure was very effective to automatic thresholding of images with local variations of illumination. Brainard *et al.* [11] showed that it was possible to design the sensor spectral responsivities so that the vector direction of sensor responses might not depend upon the illuminant. They also introduced the concept about black illuminant that some changes in illumination cause no variation in the sensor responses. However, there have been no studies for calibrating the color information distorted by vision system components.

Based on the theory of image formation, the amounts of RGB variations associated with an error source change with the spectral reflectance characteristics of objects in an image. Also, different error sources might cause the same variations in output RGB color values. Therefore, it is difficult to separate error sources and their associated amounts of RGB variations from output RGB values of arbitrary objects in images. It is assumed in this study that a standardized color device, like color charts used for television adjustment, is included in images with objects for color calibration. If the scene has dynamically changing conditions affecting the appearance of objects, color calibration should be performed in every image.

One color standard that is commercially available is the color-rendition chart developed by McCamy *et al.* [12]. One chart has 24 color patches characterized by the different spectral responses. Six patches are different neutral grays from black to white; the spectral responses of these patches are constant at all wavelengths in the visible spectrum and differ only by a scalar multiplier. Each color patch in the chart is about 5 cm square. The size of color patches can be adjusted as the scene design.

Chang [13] developed a method of characterizing a color vision system based on the theory of image formation in machine vision. His method was to estimate the spectral characteristics of vision system components and the relationship in conversion process between input quantum power and output digital values. When the characteristics of a vision system are known, one can calculate the theoretical RGB values of a color with the known spectral reflectance. The theoretical RGB values represent the basic quantitative color characteristic in RGB domain and do not include RGB corrections. Hence, one can use the theoretical RGB values as a standard measure to estimate the RGB corrections in a particular image. The difference between the theoretical and the actual RGB values of a color is the RGB errors involved in the color. When the color chart is included in an image with objects of interest, the RGB errors of 24 color patches provide information about the RGB variations caused by vision system components. The RGB corrections of arbitrary objects in the image are estimated from the information provided by color patches. The RGB values of objects are calibrated by the estimated RGB corrections and restored on a pixel basis.

The objectives in this study were to develop a method for calibrating variations in RGB color values caused by vision system components and to develop an automatic color calibration software procedure as a basic tool for color image analysis.

## II. An Algorithm for Color Calibration

### A. A Model of RGB Errors

For a Lambertian diffuser, the theoretical digital value of a pixel, $g_{i,t}(x, y)$ is

$$g_{i,t}(x, y) = \alpha_i \cdot \left[\int_\lambda I(\lambda; x, y) \cdot M_i(\lambda; x, y)\, d\lambda\right]^{\gamma i} + \beta_i \quad (1)$$

where the subscript of $i$ is red, green, or blue color channel, $\lambda$ is the wavelength (nm), $x$ and $y$ are the coordinates of a pixel in an image, $I(\lambda; x, y)$ is the spectral power distribution of illumination incident to the surface of an object in a scene (watt $\cdot$ m$^{-2}\cdot$ nm$^{-1}$), $M_i(\lambda; x, y)$ is the multiplication of $O(\lambda; x, y) \cdot L(x, y) \cdot F_i(\lambda) \cdot C(\lambda)$, $O(\lambda; x, y)$ is the spectral reflectance of the object, $L(\lambda; x, y)$ is the spectral attenuation of the light reflected from the object to a color filter through a lens, $F_i(\lambda)$ is the spectral transmittance of color filters and $C(\lambda)$ is the spectral sensitivity of image sensors, $\alpha_i$ is the slope related to amplification and quantization in camera electronics or frame grabber, $\beta_i$ is the intercept related to dark current, and $\gamma_i$ is the gamma correction of the camera electronics. The gamma correction $\gamma_i$ can be set to one for each color channel when a camera can be adjusted to respond linearly.

The actual RGB values of colors in an image may contain some errors caused by the vision system components. The RGB errors can come from various error sources; for example, the change in the intensity and the color temperature of illumination, dark current due to thermal fatigue of the sensors, or the spectral transmittance of color filters with time. Other known error sources have been depicted in the literature [1], [14]. Error sources might be random and have a major or minor effect on the digital values of colors in an image. However, it is difficult to exactly model and classify all error sources and their effects on the RGB values of colors. In addition, calibrating the RGB errors contained in an image is very important in color image analysis to obtain a reliable result of the analysis.

This study concentrates on estimating and removing the RGB errors caused by vision system components without specifying error sources and their effects. Also, the calibration scheme in this study does not account for variations in the spectral characteristics of individual pixels. Thus, in this study it is assumed that the RGB errors are comprehensively categorized into two classes based on the theory of image formation in machine vision—multiplicative and additive errors. The additive errors are linear shifts of RGB values caused by vision system components, such as the gray-level shift [6]. The amount of additive errors for each color channel might be different but are assumed to be the same for the color channel in an image. The multiplicative errors are influenced by the spectral characteristics of the vision system components or the amplification of signals, for example, mutual illumination [16], the change of color temperature of illumination with time, and related factors. Therefore, the amount of multiplicative errors are related to the spectral reflectance of colors contained in an image.

When additive and multiplicative RGB errors exist in an image, the actual digital value $g_{i,a}(x, y)$ is modeled as follows:

$$g_{i,a}(x, y) = \alpha_i^e \cdot \left[\int_\lambda I^e(\lambda; x, y) \cdot M_i^e(\lambda; x, y)\, d\lambda\right]^{\gamma i} + \beta_i + \delta E_i \quad (2)$$

where $M_i^e(\lambda; x, y)$ is $O(\lambda; x, y) \cdot L^e(x, y) \cdot F_i^e(\lambda) \cdot C^e(\lambda)$, and $\delta E_i$ is the sum of the additive errors. The superscript "$e$" in (2) means that the corresponding system component might have a variation in its characteristic and generate multiplicative RGB errors. In an image, more than one error source can cause the RGB errors at the same time. Note that, when a system component is characterized by a spectral function of $\lambda$, the changed characteristic of the component is another spectral function of $\lambda$ and can be represented with the superscript "$e$." Thus, for example, if there is a variation in the color temperature or intensity of illumination, $I(\lambda; x, y)$ in (1) is changed to $I^e(\lambda; x, y)$ in (2). The $\alpha_i^e$ in the equation represents a variation in amplification or quantization.

### B. Correction of Nonuniform Illumination

In calibrating RGB errors caused by vision system components, it is important that illumination is uniform over the scene. The error caused by any vision system component exclusively increases or decreases the RGB values at all positions of an image. However, the error caused by nonuniformity of illumination arbitrarily changes the RGB values as local variations of illumination in an image. Hence, the nonuniformity of illumination causes two problems in color calibration. One problem is that the RGB errors associated with the nonuniformity of illumination can be misinterpreted as the ones caused by a vision system component. The other problem is that, if the direction of error correction is not accorded with the nonuniformity of illumination, the RGB errors are not corrected within local regions of the image. Because it is difficult to obtain uniform illumination over the scene, color calibration must correct for nonuniform illumination.

The spectral power distribution (SPD) of illumination at an arbitrary position of $(x_p, y_p)$ in an image, $I(\lambda; x_p, y_p)$ is expressed as

$$I(\lambda; x_p, y_p) = r(x_p, y_p) \cdot I(\lambda; x_m, y_m) \tag{3}$$

where $I(\lambda; x_m, y_m)$ is the SPD of illumination at the middle position of $(x_m, y_m)$, and $r(x_p, y_p)$ is the nonuniformity factor of illumination defined as the ratio of $I(\lambda; x_p, y_p)$ to $I(\lambda; x_m, y_m)$. One can assume that the color temperature of $I(\lambda; x_p, y_p)$ is identical to that of $I(\lambda; x_m, y_m)$, and $r(x_p, y_p)$ is a function of the position. It depends on one's decision to select a standard SPD of illumination in an image. However, it is natural to consider the SPD at the middle position as a standard because, in many cases, objects would be located in the middle area of the image.

If an image contains only an object, such as a reflectance panel, parallel to the image plane, the actual digital value $g_{i,a}(x_m, y_m)$ at the middle position is

$$\begin{aligned} g_{i,a}(x_m, y_m) &= \\ &\alpha_i^e \cdot \left[\int_\lambda I^e(\lambda; x_m, y_m) \cdot M_i^e(\lambda; x_m, y_m)\, d_\lambda\right]^{\gamma i} \\ &+ \beta_i + \delta E_i \end{aligned} \tag{4}$$

where $M_i^e(\lambda; x_m, y_m)$ is $O(\lambda) \cdot L^e(x_m, y_m) \cdot F_i^e(\lambda) \cdot C^e(\lambda)$. It is assumed in (4) that there exist additive and multiplicative RGB errors in the test image. With (3), the actual digital value $g_{i,a}(x_p, y_p)$ at an arbitrary position is

$$\begin{aligned} &g_{i,a}(x_p, y_p) \\ &= \alpha_i^e \cdot \left[\int_\lambda I^e(\lambda; x_p, y_p) \cdot M_i^e(\lambda; x_p, y_p)\, d_\lambda\right]^{\gamma i} \\ &\quad + \beta_i + \delta E_i \\ &= r(x_p, y_p)^{\gamma i} \cdot \alpha_i^e \\ &\quad \cdot \left[\int_\lambda I^e(\lambda; x_m, y_m) \cdot M_i^e(\lambda; x_p, y_p)\, d_\lambda\right]^{\gamma i} \\ &\quad + \beta_i + \delta E_i \end{aligned} \tag{5}$$

where $M_i^e(\lambda; x_p, y_p)$ is $O(\lambda) \cdot L^e(x_p, y_p) \cdot F_i^e(\lambda) \cdot C^e(\lambda)$. Combining (4) and (5), one can obtain the nonuniformity factor of $r(x_p, y_p)$ in terms of the digital values in the image as follows:

$$\begin{aligned} r(x_p, y_p) = &\frac{L^e(x_m, y_m)}{L^e(x_p, y_p)} \\ &\cdot \frac{[g_{i,a}(x_p, y_p) - \beta_i - \delta E_i]^{\gamma i}}{[g_{i,a}(x_m, y_m) - \beta_i - \delta E_i]^{\gamma i}}. \end{aligned} \tag{6}$$

The ratio of $L^e(x_m, y_m)/L^e(x_p, y_p)$ is calculated by $\cos^4\theta(x_m, y_m)/\cos^4\theta(x_p, y_p)$ because $L^e(x, y) = (1/4) \cdot (d^e/f^e)^2 \cdot \cos^4\theta(x, y)$ where $d^e$ is the opening diameter of lens at an aperture, $f^e$ is the focal length of lens, and $\theta(x, y)$ is the optical axis offset at the position of $(x, y)$ [15]. Thus, the nonuniformity of illumination can be corrected by multiplying the reciprocal of the nonuniformity factor $r(x_p, y_p)$ to the RGB values from which the linear terms of $\beta_i$ and $\delta E_i$ are deducted at each position.

To apply (6), the additive RGB errors, $\delta E_i$ involved in test images should be evaluated. One can estimate the additive RGB errors in test images by locating a small black patch, whose spectral reflectance is close to zero in the visible spectrum, in the middle area of the image. In this case, the actual digital value of the black patch $g_{i,b/a}(x_m, y_m)$ is

$$\begin{aligned} g_{i,b/a}(x_m, y_m) &= \\ &\alpha_i^e \cdot \left[\int_\lambda I^e(\lambda; x_m, y_m) \cdot M_{i,b}^e(\lambda; x_m, y_m)\, d_\lambda\right]^{\gamma i} \\ &+ \beta_i + \delta E_i \end{aligned} \tag{7}$$

and the theoretical digital value of black patch $g_{i,b/t}(x_m, y_m)$ is

$$\begin{aligned} g_{i,b/t}(x_m, y_m) &= \\ &\alpha_i \cdot \left[\int_\lambda I(\lambda; x_m, y_m) \cdot M_{i,b}(\lambda; x_m, y_m)\, d\lambda\right]^{\gamma i} + \beta_i. \end{aligned} \tag{8}$$

Subtracting the theoretical digital value from the actual one, the additive error in the test image $\delta E_i$ approximates

$$\delta E_i \approx g_{i,b/a}(x, y) - g_{i,b/t}(x, y). \tag{9}$$

It is noted that the multiplicative errors are negligible in black patch due to its small spectral reflectance.

There are two technical recommendations in evaluating the nonuniformity of illumination. One is to use white background (a white reflectance panel) because the spectral reflectance of white is high enough to apparently expose the nonuniformity of illumination in the scene. To preserve the nonuniformity of illumination in test images, RGB values of white background should be under the saturation level. In such an illumination configuration, RGB values of a black patch contained in test images is small enough to neglect the effect of multiplicative errors on the black patch. The other is to model the change of $r(x, y)$ in the scene by $x$ and $y$ spatial coordinates on the image. Such a model can save computer memory in pixel-based correction of nonuniform illumination, and also provide a way to adjust the size of the reflectance panel in a scene. For example, it is possible to evaluate the nonuniformity of illumination in a broad scene by measuring the RGB values of small white patches at several arbitrary positions in the scene.

### C. Correction of Additive RGB Errors

As mentioned earlier, the color calibration procedure requires that a color chart is included in images. One can estimate the additive RGB errors in an image using the actual and the theoretical RGB values of any two color patches whose spectral reflectance differ only by a multiplier. The selection of two color patches can be arbitrary and only depends upon the relationship between their spectral reflectance. From a practical standpoint, it is not always possible to locate the color chart at the middle position of images. The method developed in this section is a generalized way to evaluate the additive RGB errors, different from the approximation used in (9), when the color chart is located at a random position in the image under nonuniform illumination.

The color chart contains a white and a black patch.[1] The spectral reflectance of white patch is a multiplier of that of black patch. Then $O_w(\lambda) = k_{w/b} \cdot O_b(\lambda)$ where the subscripts of $b$ and $w$ represent the black and the white patch and$k_{w/b}$ is the multiplier between the spectral reflectance of white and black patch. First, one can evaluate the multiplier $k_{w/b}$ using the theoretical digital values of the two patch. It is assumed that there are no RGB errors in the theoretical digital values of colors with known spectral reflectance [13]. When the white and black patch are respectively located at different positions of $(x_w, y_w)$ and $(x_b, y_b)$ in an image, the multiplication of spectral functions for white patch, $M_{i,w}(\lambda; x_w, y_w)$, can be expressed from (1) as

$$M_{i,w}(\lambda; x_w, y_w) = k_{w/b} \cdot L_{w/b} \cdot M_{i,b}(\lambda; x_b, y_b) \tag{10}$$

where $L_{w/b} = L(x_w, y_w)/L(x_b, y_b) = \cos^4\theta(x_w, y_w) / \cos^4\theta(x_b, y_b)$, $M_{i,b}(\lambda; x_b, y_b)$ is the multiplication of spectral functions for black patch. Thus, the theoretical digital values of $g_{i,b/t}(x_b, y_b)$ for black patch and $g_{i,w/t}(x_w, y_w)$ for white patch are, respectively

$$\begin{aligned} g_{i,b/t}&(x_b, y_b) \\ &= \alpha_i \cdot \left[\int_\lambda I(\lambda; x_m, y_m) \cdot M_{i,b}(\lambda; x_b, y_b)\, d\lambda\right]^{\gamma i} + \beta_i \end{aligned} \tag{11}$$

$$\begin{aligned} g_{i,w/t}&(x_w, y_w) \\ &= \alpha_i \cdot \left[\int_\lambda I(\lambda; x_m, y_m) \cdot M_{i,w}(\lambda; x_w, y_w)\, d\lambda\right]^{\gamma i} + \beta_i \\ &= \alpha_i \cdot \left[k_{w/b} \cdot L_{w/b} \cdot \int_\lambda I(\lambda; x_m, y_m)\right. \\ &\qquad \left. \cdot\, M_{i,b}(\lambda; x_b, y_b)\, d\lambda\right]^{\gamma i} + \beta_i. \end{aligned} \tag{12}$$

[1] The following formulation was also applied for a gray and a black patch if the relationship between the spectral reflectance of two color patches can be expressed by a multiplier.

Arranging the equations of (11) and (12), we have

$$k_{w/b} = \frac{1}{L_{w/b}} \cdot \left[\frac{g_{i,w/t}(x_w, y_w) - \beta_i}{g_{i,b/t}(x_b, y_b) - \beta_i}\right]^{1/\gamma i}. \tag{13}$$

Based on (13), one can experimentally obtain the averaged multiplier between the spectral reflectance of white and black patch in the visible spectrum.

When the relationship between the spectral reflectance of white and black patch is known, the additive RGB errors are estimated by using the actual RGB values of two patches. If nonuniform illumination exists in the scene, the actual digital values of $g_{i,b/a}(x_b, y_b)$ for black patch and $g_{i,w/a}(x_w, y_w)$ for white patch are

$$\begin{aligned} g_{i,b/a}&(x_b, y_b) \\ &= \alpha_i^e \cdot \left[\int_\lambda r(x_b, y_b) \cdot I^e(\lambda; x_m, y_m)\right. \\ &\qquad \left. \cdot\, M_{i,b}^e(\lambda; x_b, y_b) d_\lambda\right]^{\gamma i} + \beta_i + \delta E_i \end{aligned} \tag{14}$$

$$\begin{aligned} g_{i,w/a}&(x_w, y_w) \\ &= \alpha_i^e \cdot \left[\int_\lambda r(x_w, y_w) \cdot I^e(\lambda; x_m, y_m)\right. \\ &\qquad \left. \cdot\, M_{i,w}^e(\lambda; x_w, y_w) d_\lambda\right]^{\gamma i} + \beta_i + \delta E_i \\ &= \alpha_i^e \cdot \left[\int_\lambda r(x_w, y_w) \cdot k_{w/b} \cdot L_{w/b}^e \cdot I^e(\lambda; x_m, y_m)\right. \\ &\qquad \left. \cdot\, M_{i,b}^e(\lambda; x_b, y_b) d_\lambda\right]^{\gamma i} + \beta_i + \delta E_i \end{aligned} \tag{15}$$

where $L_{w/b}^e = L^e(x_w, y_w)/L^e(x_b, y_b) = L(x_w, y_w) / L(x_b, y_b) = \cos^4\theta(x_w, y_w)/\cos^4\theta(x_b, y_b)$. Combining (14) and (15), the additive RGB errors in the image, $\delta E_i$ are given in (16), shown at the bottom of the page, where $k_{w/b}$ and $r(x, y)$ are evaluated by (13) and (6), respectively. The $\beta_i$ is the output digital value in images when input quantum power at image sensors is set to zero [13], [14]. It should be noted that the term of $L_{w/b}^e$ can be technically set to one by locating the white and the black patch at nearly same position in the image. The additive RGB errors are corrected by simply subtracting $\delta E_i$ from the RGB values at every pixel in the image.

### D. Correction of Multiplicative RGB Errors

The multiplicative RGB errors for an arbitrary color in images depend on its unknown spectral reflectance. For example, the ideal black with the spectral reflectance of zero in the visible spectrum does not contain multiplicative RGB errors. Also, if the variation in illumination occurs only in blue waveband, the colors whose spectral reflectance are inclined

$$\delta E_i = \frac{\left\{k_{w/b} \cdot L_{w/b}^e \cdot \left[\dfrac{r(x_w, y_w)}{r(x_b, y_b)}\right]\right\}^{\gamma i} \cdot [g_{i,b/a}(x_b, y_b) - \beta_i] - [g_{i,w/a}(x_w, y_w) - \beta_i]}{\left\{k_{w/b} \cdot L_{w/b}^e \cdot \left[\dfrac{r(x_w, y_w)}{r(x_b, y_b)}\right]\right\}^{\gamma i} - 1} \tag{16}$$

to green or red waveband (such as pure red) barely reflect the corresponding multiplicative error. Therefore, it is important to obtain the information about the spectral reflectance of a color before estimating its multiplicative RGB errors.

The spectral reflectance of a color is surveyed by comparing its actual RGB values with those of standard colors in an image. Again, assume that additive and multiplicative RGB errors exist in an image under nonuniform illumination. The actual digital value of a color with unknown spectral reflectance at a position of $(x_u, y_u)$, $g_{i,u/a}(x_u, y_u)$ is

$$g_{i,u/a}(x_u, y_u) = \alpha_i^e \cdot \left[ \int_\lambda r(x_u, y_u) \cdot I^e(\lambda; x_m, y_m) \cdot M_{i,u}^e(\lambda; x_u, y_u)\, d\lambda \right]^{\gamma i} + \beta_i + \delta E_i \tag{17}$$

where $r(x_u, y_u)$ is the nonuniformity factor of illumination at the position of $(x_u, y_u)$, $M_{i,u}^e(\lambda; x_u, y_u)$ is $O_u(\lambda) \cdot L^e(x_u, y_u) \cdot F_i^e(\lambda) \cdot C^e(\lambda)$. Based on (17), a nonlinear transformation for the RGB values of the color, $T_{i,u/a}$ can be defined in (18), shown at the bottom of the page, where $r(x_u, y_u)$ and $L^e(x_u, y_u)$ in (17) are cancelled out in (18). Similarly, the nonlinear transformation for the RGB values of a standard color at the position of $(x_c, y_c)$, $T_{i,c/a}$ is shown in (19), at the bottom of the page. The transformation $T_i$ is a modified form of chromaticity representing the ratio of each value to the linear sum of RGB values.

Equations (18) and (19) say that if the spectral reflectance of the arbitrary color is approximately related by a multiplier of that of a standard color in the image [that is, $O_u(\lambda) \approx k_{u/c} \cdot O_c(\lambda)$], the transformations of $T_{i,u/a}$ and $T_{i,c/a}$ are almost identical even though multiplicative RGB errors exist. The reason is that the multiplier of $k_{u/c}$ is also cancelled out in (18), as $r(x_u, y_u)$ and $L^e(x_u, y_u)$. Such a fact implies that the multiplicative RGB errors for an arbitrary color will follow those for the standard color due to the similarity between the spectral reflectance of two colors.

To check the similarity between the spectral reflectance of an arbitrary color and a standard color in the image [17], one can apply the Euclidean metric for the distance between $T_{i,u/a}$ and $T_{i,c/a}$ in the transformed color space of $T$, as follows:

$$d(T_{i,u/a}, T_{i,c/a}) = [(T_{R,u/a} - T_{R,c/a})^2 + (T_{G,u/a} - T_{G,c/a})^2]^{1/2} \tag{20}$$

where $T_b = 1 - (T_R + T_G)$. The small distance between $T_{i,u/a}$ and $T_{i,c/a}$ reflects the closeness between the spectral characteristics of two colors. It is, however, noted that the transformation of $T_i$ contains no information about the magnitude of the spectral reflectance of the arbitrary color.

When a standard color is selected by (20), the magnitude of the spectral reflectance of the arbitrary color can be estimated from the ratio between the actual RGB values of the arbitrary and the selected standard color. For each color channel, a multiplier between the spectral reflectance of two colors, $K_{i,u/c}$, is defined as follows:

$$\begin{aligned} K_{i,u/c} &= k_{i,u/c} \cdot \frac{L^e(x_u, y_u)}{L^e(x_c, y_c)} \\ &= \frac{r(x_c, y_c)}{r(x_u, y_u)} \cdot \left[ \frac{g_{i,u/a}(x_u, y_u) - \beta_i - \delta E_i}{g_{i,c/a}(x_c, y_c) - \beta_i - \delta E_i} \right]^{1/\gamma i} \end{aligned} \tag{21}$$

where $k_{i,u/c}$ is the real multiplier between the spectral reflectance of two colors, namely $O_{i,u}(\lambda) \approx k_{i,u/c} \cdot O_{i,c}(\lambda)$.

Note in (21) that the multiplier between the spectral reflectance of two colors is evaluated separately for each color channel. In reality, the spectral reflectance of an arbitrary color can not be precisely related by a multiplier of that of a standard color in the visible spectrum. However, separating the visible spectrum to RGB regions provides a good estimation for the relationship between the arbitrary and the standard color. Even though there might be some variations in the spectral reflectance of two colors, such variations can be neglected in their output digital values. In addition, (21) reflects the fact, from the multiplier of $K_{i,u/c}$, that the multiplicative RGB errors change with position in the image. Multiplicative errors of an arbitrary color in the image are obtained by multiplying $K_{i,u/c}$ to those of the selected standard color for each color channel.

$$\begin{aligned} T_{i,u/a} &= \frac{[g_{i,u/a}(x_u, y_u) - \beta_i - \delta E_i]^{1/\gamma i}}{\Sigma_{\mathrm{RGB}}[g_{j,u/a}(x_u, y_u) - \beta_j - \delta E_j]^{1/\gamma j}} \\ &= \frac{(\alpha_i^e)^{1/\gamma i} \cdot \left[ \int_\lambda I^e(\lambda; x_m, y_m) \cdot O_u(\lambda) \cdot F_i^e(\lambda) \cdot C^e(\lambda)\, d\lambda \right]}{\Sigma_{\mathrm{RGB}} (\alpha_j^e)^{1/\gamma j} \cdot \left[ \int_\lambda I^e(\lambda; x_m, y_m) \cdot O_u(\lambda) \cdot F_i^e(\lambda) \cdot C^e(\lambda)\, d\lambda \right]} \end{aligned} \tag{18}$$

$$\begin{aligned} T_{i,c/a} &= \frac{[g_{i,c/a}(x_c, y_c) - \beta_i - \delta E_i]^{1/\gamma i}}{\Sigma_{\mathrm{RGB}}[g_{j,c/a}(x_c, y_c) - \beta_j - \delta E_j]^{1/\gamma j}} \\ &= \frac{(\alpha_i^e)^{1/\gamma i} \cdot \left[ \int_\lambda I^e(\lambda; x_m, y_m) \cdot O_c(\lambda) \cdot F_i^e(\lambda) \cdot C^e(\lambda)\, d\lambda \right]}{\Sigma_{\mathrm{RGB}} (\alpha_j^e)^{1/\gamma j} \cdot \left[ \int_\lambda I^e(\lambda; x_m, y_m) \cdot O_c(\lambda) \cdot F_i^e(\lambda) \cdot C^e(\lambda)\, d\lambda \right]} \end{aligned} \tag{19}$$

In calibrating the RGB errors caused by the vision system components, the final purpose is to recover the theoretical RGB values of a color with unknown spectral reflectance in an image. From the above equations, the theoretical digital value of the arbitrary color at the position of $(x_u, y_u)$, $g_{i,u/t}(x_u, y_u)$ is

$$\begin{aligned} g_{i,u/t}&(x_u, y_u) \\ &= g_{i,u/a}(x_u, y_u) - (\text{the additive errors} \\ &\quad + \text{the multiplicative errors}) \\ &= \alpha_i \cdot \left[\int_\lambda I(\lambda; x_u, y_u) \cdot M_{i,u}(\lambda; x_u, y_u)\, d\lambda\right]^{\gamma i} + \beta_i \\ &= \alpha_i \cdot \left\{\int_\lambda I(\lambda; x_m, y_m) \cdot k_{i,u/c} \cdot \left[\frac{L(x_u, y_u)}{L(x_c, y_c)}\right]\right. \\ &\quad \left. \cdot\ M_{i,c}(\lambda; x_c, y_c)\, d\lambda\right\}^{\gamma i} + \beta_i \\ &= K_{i,u/c}^{\gamma i} \cdot g_{i,c/t}(x_c, y_c) + (1 - K_{i,u/c}^{\gamma i}) \cdot \beta_i \end{aligned} \tag{22}$$

where $g_{i,c/t}(x_c, y_c)$ is the theoretical digital value of the standard color selected by (20), and $K_{i,u/c}$ is

$$\begin{aligned} K_{i,u/c} &= k_{i,u/c} \cdot \frac{L^e(x_u, y_u)}{L^e(x_c, y_c)} \\ &= k_{i,u/c} \cdot \frac{L(x_u, y_u)}{L(x_c, y_c)}. \end{aligned}$$

Several observations can be made for this color calibration method. The first is that the calibration scheme is based on the assumption that the spectral reflectance of $O(\lambda)$ changes very smoothly from one color to the other. For example, the spectral characteristics of "orange" and "yellow" are similar except that the spectral reflectance of "orange" is more inclined to red waveband. If the illumination varies in red waveband, both colors will reflect the effect of the variation in their actual RGB values. Thus, a relationship between the actual RGB values of two colors contains the information about their multiplicative RGB errors. Second, the calibration scheme does not account for the changes in the spectral sensitivity of individual pixels. To remove any abrupt change in the characteristic of a pixel, a window-averaging, such as 3×3 averaging of RGB values, can be applied to the calibration scheme. Finally, this color calibration preserves the variation in the RGB values resulting from the change in geometry of objects, which can be useful information in a particular color image analysis. Basically, the change in the geometry of objects would not belong to the errors caused by the vision system components.

This color calibration method can be used as a preprocessing tool for various color image analyses. For instance, in the case that one wants to observe the color changes with time, such as modeling of plant growth or grading of product quality based on a color, the method will remove the RGB variation of colors caused by vision system components and only color characteristics will emerge that are intended for analysis. The theoretical digital values of standard colors with known spectral reflectance can be also substituted by their actual values at an arbitrary time when the color analysis starts. Such substitutions will change the calibration scheme to a normalization procedure for color analysis at the starting time of the analysis.

## III. Experiments

A lighting chamber with four 50-W direct current (dc) halogen lamps and four white reflectors was designed for diffuse illumination. The input dc voltage was controlled by a variable dc-voltage regulator. The dc-voltage regulator had a voltage indicator with a 0.5-V interval. The actual voltage range that the regulator could control was 4–23 V for this lighting chamber. The distance between illumination sources and objects was fixed to 1 m based on the size of the color chart in test images. A camera lens with a focal length of 24 mm, a Sony XC-711 CCD color camera, and an ATvista color image board (Truevision Inc., Indianapolis, IN) were used for the study. The aperture of the camera lens ranged from f2–f16 with seven steps.

The color calibration algorithm was tested separately under uniform and nonuniform illumination. The calibration method contained an algorithm for correcting nonuniformity of illumination in the scene. To enhance the effectiveness of the calibration algorithm in correcting multiplicative and additive RGB errors caused by vision system components, nonuniformity factors under uniform illumination were assumed to be one at all positions in test images. A comprehensive test for the calibration method, including the algorithm for correcting nonuniformity of illumination in the scene, was performed under nonuniform illumination.

Some selected color patches were located at random positions as arbitrary objects in test images. The theoretical RGB values of color patches at input voltage of 20 V and lens aperture of f4 were used as a standard measure for estimating the RGB errors. The location of the color chart was fixed at the upper left corner in test images. It was assumed that the RGB errors were generated by changing the input voltage from 20 V to 17 V at the same lens aperture. Reducing the input voltage into the illumination system caused change in color temperature as well as the intensity of illumination. Also, since the vision system used in this study had gray-level shift defined as an additive error, test images contained multiplicative and additive RGB errors together. The nonuniform illumination was generated by biasing two halogen lamps in the lighting chamber.

Based upon the developed calibration scheme, a program for color calibration was written in Microsoft 6.0 C language (Microsoft Corp., Redmond, WA). As a prerequisite procedure for color calibration, the user provides the characteristics of the vision system, $\beta_i$ and $\gamma_i$ in (1), and the theoretical RGB values of standard colors using given system configuration [13]. The program contains an algorithm for evaluating the nonuniformity factor of illumination by using the white background with a black patch at the middle position of test images. The nonuniformity of illumination is modeled as a polynomial function of image spatial coordinates of $x$ and $y$ from first to third order in this study. The program returns the statistics for the model of the nonuniform illumination.

One can fix the positions of standard color patches in images before starting color calibration. For the case that the positions of patches change in every image, the program provides a tool for locating the standard color patches at every calibration.

TABLE I
RESULTS OF COLOR CALIBRATION UNDER UNIFORM ILLUMINATION

| Patch Number | RGB values[1] before calibration | RGB values after calibration | Theoretical[2] RGB values | Residual[3] RGB errors |
|---|---|---|---|---|
| 2. light skin | (92, 55, 44) | (144, 83, 71) | (139, 77, 65) | (5, 6, 6) |
| 3. blue sky | (41, 41, 44) | (47, 48, 59) | (51, 53, 66) | (-4, -5, -7) |
| 4. foliage | (36, 35, 25) | (40, 39, 30) | (41, 41, 29) | (-1, -2, 1) |
| 6. bluish green | (60, 71, 61) | (79, 105, 100) | (80, 107, 103) | (-1, -2, -3) |
| 7. orange | (97, 46, 27) | (145, 61, 28) | (144, 60, 27) | (1, 1, 1) |
| 9. moderate red | (81, 34, 31) | (118, 38, 35) | (119, 38, 35) | (-1, 0, 0) |
| 10. purple | (34, 27, 28) | (41, 27, 33) | (38, 25, 30) | (3, 2, 3) |
| 13. blue | (27, 26, 37) | (30, 30, 54) | (26, 26, 51) | (4, 4, 3) |
| 14. green | (39, 49, 30) | (48, 69, 45) | (46, 68, 42) | (2, 1, 3) |
| 15. red | (71, 29, 25) | (101, 30, 26) | (98, 26, 22) | (3, 4, 4) |
| 16. yellow | (129, 84, 39) | (187, 122, 48) | (187, 122, 48) | (0, 0, 0) |
| 17. magenta | (81, 36, 39) | (112, 38, 50) | (113, 39, 52) | (-1, -1, -2) |
| 18. cyan | (33, 43, 50) | (36, 54, 80) | (36, 54, 80) | (0, 0, 0) |
| 20. neutral 8 | (104, 81, 70) | (148,119,114) | (152,122,116) | (-4, -3, -2) |

1. represents actual RGB values at 17V with gray-level shift.
2. represents theoretical RGB values at 20V without gray-level shift.
3. Residual RGB errors were obtained by deducting theoretical RGB values in 4th column from RGB values after calibration in 3rd column.

First, the averaged multiplier between the spectral reflectance of white and black patch is calculated from their theoretical RGB values. Then, the additive RGB errors are estimated by using the actual digital values of black and white patch.

Fundamentally, color calibration is performed at all pixels in the image. However, the program has a windowing function to limit color calibration to a local region of interest. The multiplicative RGB errors at each pixel are estimated by comparing the actual RGB values at the pixel with those of standard color patches. The program calculates the theoretical RGB values at the pixel and restores them in the image as error-free color values. Color calibration is automatically executed whenever a new image is acquired. In the case that a previous image stored without calibration is retrieved, it is also possible to manually calibrate the image.

## IV. RESULTS AND DISCUSSION

Table I shows the results of color calibration under uniform illumination. RGB errors were generated by changing the input voltage into the illumination system from 20 V to 17 V. In comparison with the theoretical RGB values of color patches at 20 V, the RGB errors in test images ranged from zero gray levels at patch no. 7 to 58 gray levels at patch no. 16. As shown in Table I, most RGB errors of color patches were removed after color calibration. The maximum residual error was seven gray levels at the blue value of patch no. 3. The RGB errors of some color patches (no. 4, no. 7, no. 9, no. 16, no. 17, and no. 18) were almost perfectly eliminated.

Since the Euclidean metric of (20) in the transformed color space of $T$ classified the color patches into their groups very successfully, there were little residual RGB errors caused by the misclassification of color patches. In this experiment, the nonuniformity factor was assumed to be one at every pixel. However, there was a slight nonuniformity of illumination in test images. The residual RGB errors of patch no. 2, no. 3, and no. 20 resulted from the nonuniformity of illumination. The patches of nos. 2 and 15, and the patches of nos. 3 and 20 were, respectively, located at almost the same positions in test images. Thus, the directions of residual errors in those pairs of color patches were similar for all RGB color channels. The

TABLE II
RESULTS OF COLOR CALIBRATION UNDER NONUNIFORM ILLUMINATION

| Patch Number | RGB values[1] before calibration | RGB values after calibration | Theoretical[2] RGB values | Residual[3] RGB errors |
|---|---|---|---|---|
| 2. light skin | (111, 65, 49) | (146, 81, 69) | (139, 77, 65) | (7, 4, 4) |
| 3. blue sky | (45, 45, 49) | (56, 57, 73) | (51, 53, 66) | (5, 4, 7) |
| 4. foliage | (37, 36, 25) | (46, 45, 31) | (41, 41, 29) | (5, 4, 2) |
| 6. bluish green | (62, 72, 63) | (83, 112, 107) | (80, 107, 103) | (3, 5, 4) |
| 7. orange | (98, 45, 27) | (146, 61, 28) | (144, 60, 27) | (2, 1, 1) |
| 9. moderate red | (79, 33, 30) | (114, 38, 35) | (119, 38, 35) | (-5, 0, 0) |
| 10. purple | (32, 26, 27) | (36, 24, 28) | (38, 25, 30) | (-2, -1, -2) |
| 13. blue | (25, 24, 34) | (23, 24, 44) | (26, 26, 51) | (-3, -2, -7) |
| 14. green | (35, 44, 28) | (40, 59, 37) | (46, 68, 42) | (-6, -9, -5) |
| 15. red | (63, 25, 23) | (89, 25, 23) | (98, 26, 22) | (-9, -1, 1) |
| 16. yellow | (127, 83, 38) | (183, 120, 47) | (187, 122, 48) | (-4, -2, -1) |
| 17. magenta | (84, 38, 42) | (117, 41, 54) | (113, 39, 52) | (4, 2, 2) |
| 18. cyan | (34, 47, 55) | (38, 58, 87) | (36, 54, 80) | (2, 4, 7) |
| 20. neutral 8 | (123, 93, 82) | (164, 130, 123) | (152, 122, 116) | (12, 8, 7) |

1. represents actual RGB values at 17V with gray-level shift under nonuniform illumination.
2. represents theoretical RGB values at 20V without gray-level shift under uniform illumination.
3. Residual RGB errors were obtained by deducting theoretical RGB values in 4th column from RGB values after calibration in 3rd column.

color patches whose RGB values were small (nos. 10 and 13) contained the residual errors caused by the overestimation of the multipliers between two patches. Because the unit change of one gray level was significantly weighed as the RGB values were decreasing, the multipliers estimated from (21) were easily exaggerated in those patches.

Table II shows the results of color calibration under nonuniform illumination that was generated by biasing two halogen lamps in the lighting chamber. In comparison with illumination at the middle position in test images, visually, some patches (no. 2, no. 3, no. 4, no. 18, and no. 20) were in the bright region while others patches (no. 9, no. 10, no. 13, no. 14, and no. 15) were in the dark region. The RGB errors were, again, generated by changing the input voltage from 20 V to 17 V at f4 as the above experiment. The nonuniformity of illumination was modeled as second-order polynomial function of image spatial coordinates, $x$ and $y$.

The RGB errors in test images ranged from zero gray level at patch no. 7 to 60 gray levels at patch no. 16, as shown in Table II. The calibration method removed most RGB errors of color patches again in the changed condition. The residual RGB error increased somewhat up to 12 gray levels at the red value of patch no. 20. Note that the residual errors of patches in the bright region were positive, while those in the dark region were negative for all RGB color channels. When the nonuniformity of illumination was not corrected, the multipliers between two patches were underestimated in the dark region while overestimated in the bright region. Such a fact showed that the residual RGB errors in this experiment were mainly caused by the second-order polynomial model for the nonuniformity factor of illumination. The above experiments suggested that a better result for color calibration could be achieved when the residual nonuniformity of illumination in the image was removed.

## V. Summary and Conclusions

An algorithm for calibrating the variations in RGB color values caused by vision system components was developed and tested in this study. The calibration scheme concentrated on comprehensively estimating and removing the RGB errors without specifying error sources and their effects. The algorithm was based upon the use of a standardized color chart for color calibration. The RGB errors in color images were categorized into multiplicative and additive errors, according to the theory of image formation. The RGB errors of arbitrary colors in an image were estimated from the RGB errors of standard colors contained in the image. The color calibration method also contained an algorithm for correcting the nonuniformity of illumination in the scene. The RGB errors of arbitrary colors in test images were almost completely removed after color calibration. The maximum residual error was seven gray levels under uniform illumination and 12 gray levels under nonuniform illumination. Most residual RGB errors were caused by residual nonuniformity of illumination in images. The test results showed that the developed method was effective in correcting the variations in RGB color values caused by vision system components. Also, it was suggested that a better result for color calibration could be achieved when the residual nonuniformity of illumination in the image was removed.

## References

[1] J. H. Tappan, M. E. Wright, and F. E. Sistler, "Error sources in a digital image analysis system," *Comput. Electron. Agriculture,* vol. 2, pp. 109–118, 1987.
[2] L. A. Spomer and M. A. L. Smith, "Image analysis for biological research: camera influence on measurement accuracy," *Intell. Instrum. Comput.,* pp. 201–215, 1988.
[3] Y. Tao, C. T. Morrow, P. H. Heinemann, and J. H. Sommer, "Automated machine vision inspection of potatoes," ASAE paper no. 90-3531, Chicago, IL, 1990.
[4] I. S. Ahmad and J. F. Reid, "Computer vision technique for detecting color changes in stressed corn," ASAE paper no. 91-3052, Albuquerque, NM, 1991.
[5] A. A. Sawchuk, "Real-time correction of intensity nonlinearities in imaging systems," *IEEE Trans. Comput.,* vol. 26 no. 1, pp. 34–39, 1977.
[6] J. McClellan, "Characterization and correction of image acquisition system response for machine vision," *SPIE Optics, Illuminat., Image Sensing Machine Vis. IV,* vol. 1194, pp. 62–73, 1989.
[7] B. G. Crowther and C. M. U. Neale, "Calibration of multispectral video imagery," in *Proc. Nat. Symp. Automat. Agriculture 21st Cent.,* 1992, pp. 50–58.
[8] J. Ho, B. V. Funt, and M. S. Drew, "Separating a color signal into illumination and surface reflectance components: theory and applications," *IEEE Trans. Pattern Anal. Machine Intell.,* vol. 12, no. 10, pp. 966–977, 1990.
[9] B. A. Wandell, "The synthesis and analysis of color images," *IEEE Trans. Pattern Anal. Machine Intell.,* vol. PAMI-9, no. 1, pp. 2–13, 1987.
[10] A. Shio, "An automatic thresholding algorithm based on an illumination-independent contrast measure," *IEEE CH2752-4,* pp. 632–637, 1989.
[11] D. H. Brainard, B. A. Wandell, and W. B. Cowan, "Black light: how sensors filter spectral variation of the illuminant," *IEEE Trans. Biomed. Eng.,* vol. 36 no. 1, pp. 140–149, 1989.
[12] C. S. McCamy, H. Marcus, and J. G. Davidson, "A color-rendition chart," *Soc. Photog. Scientists Engineers,* vol. 2, no. 3, pp. 95–99, 1976.
[13] Y.-C. Chang, "A color calibration procedure for machine vision," unpublished thesis, University of Illinois at Urbana-Champaign, Urbana, IL, 1994.
[14] G. Healey and R. Kondepudy, "Radiometric CCD camera calibration and noise estimation," *IEEE Trans. Pattern Anal. Machine Intell.,* vol. 16, no. 3, pp. 267–276, 1994.
[15] D. Forsyth and A. Zisserman, "Mutual illumination," *IEEE CH2752-4,* pp. 466–473, 1989.
[16] B. K. P. Horn, *Robot Vision.* Cambridge, MA: MIT Press, 1986.
[17] G. Healey, "Color discrimination by computer," *IEEE Trans. Syst., Man, Cybern.,* vol. 19, no. 6, pp. 1613–1617, 1989.

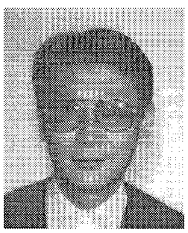

**Young-Chang Chang** (M'96) received the B.S. and M.S. degrees in agricultural engineering from Seoul National University, Seoul, Korea, in 1983 and 1985, respectively. He studied general engineering at the University of Minnesota, Minneapolis-St. Paul, from 1987 to 1988, and completed the Ph.D. degree in agricultural engineering from the University of Illinois at Urbana-Champaign in 1994.

From 1994 to 1995, he studied the application of machine vision for agricultural chemical application in the Department of Agricultural Engineering at the University of Illinois as a Research Associate. He is currently Research Associate and Instructor in the department of Agricultural Engineering at Seoul National University, Seoul, Korea. His research interest is in machine vision and includes optimization of agricultural chemical application and automation of agricultural sprayers and vehicles.

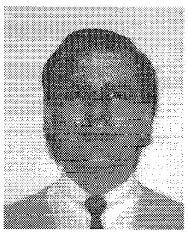

**John F. Reid** (M'94) received the B.S. and M.S. degrees in agricultural engineering from Virginia Polytechnic Institute, Blacksburg, in 1980 and 1982, respectively. He completed the Ph.D degree in 1987 on the application of machine vision for the automatic guidance of agricultural vehicles. His research interests include applications of machine vision for automated inspection and control.

Since 1986, he has been a member of the faculty in the Department of Agricultural Engineering at the University of Illinois at Urbana-Champaign. He has also been a member of the Bioengineering Faculty since 1992.

Dr. Reid is a member of ASAE and MVA.